



# Tissue Hydrogen Peroxide Concentration Can Explain the Invasiveness of Aquatic Macrophytes: A Modeling Perspective

Takashi Asaeda<sup>1,2,3\*</sup>, Md Harun Rashid<sup>4</sup> and Jonas Schoelynck<sup>5</sup>

<sup>1</sup>Hydro Technology Institute, Arco Tower, Shimo-meguro, Meguro, Tokyo, Japan, <sup>2</sup>Research and Development Center, Nippon Koei, Tsukuba, Japan, <sup>3</sup>Department of Environmental Science, Saitama University, Saitama, Japan, <sup>4</sup>Department of Agronomy, Bangladesh Agricultural University, Mymensingh, Bangladesh, <sup>5</sup>Ecosystem Management Research Group, University of Antwerp, Wilrijk, Belgium

In recent years, an invasive macrophyte, *Egeria densa*, has overwhelmingly colonized some midstream reaches of Japanese rivers. This study was designed to determine how *E. densa* has been able to colonize these areas and to assess the environmental conditions that limit or even prevent colonization. Invasive species (*E. densa* and *Elodea nuttallii*), and Japanese native species (*Myriophyllum spicatum*, *Ceratophyllum demersum*, and *Potamogeton crispus*) were kept in experimental tanks and a flume with different environmental conditions. Tissue hydrogen peroxide (H<sub>2</sub>O<sub>2</sub>) concentrations were measured responding to either individual or multiple environmental factors of light intensity, water temperature, and water flow velocity. In addition, plants were sampled in rivers across Japan, and environmental conditions were measured. The H<sub>2</sub>O<sub>2</sub> concentration increased in parallel to the increment of unpreferable levels of each abiotic factor, and the trend was independent of other factors. The total H<sub>2</sub>O<sub>2</sub> concentration is provided by the sum of contribution of each factor. Under increased total H<sub>2</sub>O<sub>2</sub> concentration, plants first started to decrease in chlorophyll concentration, then reduce their growth rate, and subsequently reduce their biomass. The H<sub>2</sub>O<sub>2</sub> concentration threshold, beyond which degradation is initiated, was between 15 and 20 μmol/gFW regardless of the environmental factors. These results highlight the potential efficacy of total H<sub>2</sub>O<sub>2</sub> concentration as a proxy for the overall environmental condition. In Japanese rivers, major environmental factors limiting macrophyte colonization were identified as water temperature, high solar radiation, and flow velocity. The relationship between the unpreferable levels of these factors and H<sub>2</sub>O<sub>2</sub> concentration was empirically obtained for these species. Then a mathematical model was developed to predict the colonization area of these species with environmental conditions. The tissue H<sub>2</sub>O<sub>2</sub> concentration decreases with increasing temperature for *E. densa* and increases for other species, including native species. Therefore, native species grow intensively in spring; however, they often deteriorate in summer. For *E. densa*, on the other hand, H<sub>2</sub>O<sub>2</sub> concentration decreases with high water temperature in summer, allowing intensive growth. High solar radiation increases the H<sub>2</sub>O<sub>2</sub> concentration, deteriorating the plant. Although the H<sub>2</sub>O<sub>2</sub> concentration of *E. densa* increases with low water temperature in winter, it can survive in deep water with low H<sub>2</sub>O<sub>2</sub> concentration due to diffused solar

## OPEN ACCESS

### Edited by:

Dana M. Infante,  
Michigan State University,  
United States

### Reviewed by:

Teresa Ferreira,  
University of Lisbon, Portugal  
Nabil I. Elsheery,  
Tanta University, Egypt

### \*Correspondence:

Takashi Asaeda  
asaeda@mail.saitama-u.ac.jp

### Specialty section:

This article was submitted to  
Freshwater Science,  
a section of the journal  
Frontiers in Environmental Science

**Received:** 30 November 2019

**Accepted:** 18 December 2021

**Published:** 29 January 2021

### Citation:

Asaeda T, Rashid MH and  
Schoelynck J (2021) Tissue Hydrogen  
Peroxide Concentration Can Explain  
the Invasiveness of Aquatic  
Macrophytes: A Modeling Perspective.  
*Front. Environ. Sci.* 8:516301.  
doi: 10.3389/fenvs.2020.516301

radiation. Currently, river rehabilitation has created a deep zone in the channel, which supports the growth and spreading of *E. densa*.

**Keywords:** alien macrophytes, hydrogen peroxide, reactive oxygen species, stress indicator, vegetation management

## INTRODUCTION

Macrophyte responses to environmental conditions are species specific, and invasive plants tend to exhibit more tolerance than native species (Zerebecki and Sorte, 2011; Bates et al., 2013). Therefore, invasive species are able to dominate or distribute in areas where native species fail to survive. Among different invasive aquatic macrophytes, *Egeria densa* is a well-known worldwide species that causes significant ecological issues in freshwater ecosystems. In Japan, *E. densa* was used as an ornamental aquarium plant in the early 19th century. However, it has escaped into natural freshwater bodies and became naturalized in the 1940s. Although *E. densa* mainly invaded lakes during the initial spreading stage in the 1970s (Kadono, 2004), this species has been recorded increasingly in many western Japanese rivers over the last two decades (MLIT, 2019). These rivers were originally nearly free of macrophytes and consisted of gravel beds and hyporheic flow (Tanida, 1984; Hauer et al., 2016). Though native species (e.g., *Myriophyllum spicatum*, *Potamogeton crispus*, and *Ceratophyllum demersum*) were colonized patchily, no large colonies were found in major rivers (Kunii, 1982; Kadono, 2004). Another alien species, *Elodea nuttallii*, also invaded at nearly the same time in 1961. However, it did not produce large colonies except for lakes and small streams. In contrast, *E. densa* spread to cover the entire river channel of major rivers. The widespread colonization of *E. densa* has led to extreme changes in these river ecosystems. After establishment, *E. densa* behaved as ecological engineers, changing the environment to their benefit (Schoelynck et al., 2012; Schoelynck et al., 2014). They reduced water flow velocity and attenuated wave energy, leading to particle settlement and, consequently, hyporheic flow capacity reduction (Madsen et al., 2001; Boano et al., 2014). It has also caused economic losses. For example, the presence of macrophytes substantially decreases the yield of Ayu (*Plecoglossus altivelis altivelis*), a grazer of benthic algae (Kawanabe, 1970). Casual monitoring between present-day abiotic conditions and plant traits, such as growth rate and biomass, is the method commonly used to evaluate the preferable habitat for macrophyte species (Barko et al., 1991; Riis et al., 2012; O'Hare et al., 2018). However, environmental conditions frequently change, and there are various types of effective factors in the natural rivers. Thus, it is difficult to apply the monitoring system in the field, particularly to derive the most influential factor.

Aquatic macrophytes growing in their natural environment often face an array of unpreferable environmental conditions, for example, too low or too high water temperatures, high flow velocity (Atapaththu and Asaeda, 2015), pollution, or substrate alteration (Asaeda et al., 2013). They can survive and propagate if the conditions remain within the plants' tolerance levels. When the environmental conditions exceed the tolerance thresholds for a considerable period of time, macrophytes become stressed, lose

their colonization capacity, and ultimately decay. However, following a short-term exposure to such conditions, they can recover, depending on the extent of the damage caused and the characteristics of the species (Weerakoon et al., 2018). Thus, the presence of a specific macrophyte species in an area depends on whether environmental factors are within their tolerance levels as well as on the duration of the exposure. When plants are subjected to unpreferable environmental conditions, reactive oxygen species (ROS) are generated in different organelles (Zaman and Asaeda, 2013; Das and Roychoudhury, 2014; Asaeda et al., 2017; Choudhury et al., 2017; Helaly et al., 2017; Parveen et al., 2017; Asaeda et al., 2018; Elsheery et al., 2020a; Elsheery et al., 2020b), which damages the plant body by the oxidative stress. Some ROS are scavenged relatively quickly by antioxidants (Omar et al., 2012), and the homogeneity of ROS in tissues is maintained by balancing the ROS and antioxidants. The balance flips over when oxidative stress surpasses the scavenging capacity of the antioxidants (Naser et al., 2016; El-Sheery, 2017; Dumont and Rivoal, 2019). Among ROS, hydrogen peroxide ( $H_2O_2$ ) is widely generated (Asada, 2006; Sharma et al., 2012), relatively stable, and can be easily measured (Satterfield and Bonnell, 1955; Zhou et al., 2006; Asaeda et al., 2020). The concentration of  $H_2O_2$  in plant tissues does not depend on a particular stress but is subjected to sum magnitude of unpreferable environmental conditions (Suzuki et al., 2014; Asaeda et al., 2020). Thus,  $H_2O_2$  concentration in the plant tissue can be used as an indicator of the physiological status of a particular macrophyte species (Smirnov and Arnaud, 2019). The system has been used for *E. densa*, which has successfully identified the channel slope that it can colonize (Asaeda et al., 2020).

The trend of  $H_2O_2$  concentration is likely as a result of a long history of acclimatization to the natural condition of a particular area; thus, it may vary widely between native and invasive species. To apply tissue  $H_2O_2$  concentration as an indicator to elucidate the intensive growth of invasive species, it is necessary to determine the relationship between  $H_2O_2$  concentration and environmental factors both for native and invasive species. The main objective of the present study is to 1) empirically determine the  $H_2O_2$  concentration generated by unpreferable conditions of abiotic environmental factors for both native and invasive species, 2) develop the model to predict the environment where these species can colonize, and 3) elucidate the reason for the overwhelming growth of *E. densa* in rivers of particular areas.

## METHODOLOGY

### Experimental Methodology

In the experiment, invasive macrophyte species (*E. densa* and *E. nuttallii*) and major Japanese species (*C. demersum*, *P. crispus*, and *M. spicatum*) were tested (MLIT, 2019). They were exposed

to different types of physical conditions, temperature, irradiance, and water flow velocity, following the range of the rivers where these species were colonized from  $\sim 8^{\circ}\text{C}$  in winter to  $30^{\circ}\text{C}$  in summer for water temperature,  $0\text{--}1,200\ \mu\text{mol}/\text{m}^2/\text{s}$  for the irradiance in water, and  $0\text{--}50\ \text{cm}/\text{s}$  for flow velocity (MLIT, 2019). For the laboratory experiments, healthy macrophyte stocks were collected from the Saba River (*E. densa*) and the Moto-Arakawa River near Tokyo (*E. nuttallii*, *C. demersum*, *P. crispus*, and *M. spicatum*). Collected plants were cleaned with water to remove debris, and any attached macro-algae were carefully separated with tweezers. The plants were then cultured in a glass tank at  $25 \pm 2^{\circ}\text{C}$  under a 12/12 h photoperiod with photosynthetically active radiation (PAR) ( $\sim 125\ \mu\text{mol}/\text{m}^2/\text{s}$  using fluorescent lamps) for over 2 months. Commercial sand ( $D_{50} < 0.1\ \text{mm}$ ) was used as a substrate, and 5% Hoagland solution was provided as the nutrient medium (Atapaththu and Asaeda, 2015). Algae were removed weekly, and algae-free plants were used in the experiments. Three types of experiments (triplicate) were conducted in total, each focusing on different combinations of environmental factors.

## Experiment 1: Water Temperature and Irradiance

A number of studies have reported that water temperature can significantly affect the abundance of different aquatic plant species (Pip, 1989; Barko et al., 1991; Lougheed et al., 2001; Pandit, 2002). An experiment was conducted to identify the increment of  $\text{H}_2\text{O}_2$  concentration of the plant tissue under different water temperatures and irradiance levels, and thereby, to make empirical relations between these factors. Several light levels ( $0\text{--}1,300\ \mu\text{mol}/\text{m}^2/\text{s}$  of PAR) were tested in small aquaria (dimensions:  $50.0\ \text{cm} \times 35.0\ \text{cm} \times 35.0\ \text{cm}$ ). Temperature level was maintained at  $10 \pm 2$  (*E. densa*),  $15 \pm 2$  (*E. densa*),  $20 \pm 2$ ,  $25 \pm 2$  (*E. densa*), and  $30 \pm 2$ ,  $35 \pm 2^{\circ}\text{C}$  using a temperature controlling system (Aquarium cooler ZC-100a, Zensui Corporation, Tokyo, Japan). PAR intensity was irradiated under natural solar radiation or using LED lights (Model LT-NLD85L-HN, OHM Electric Inc., Japan) with a 12 h light:12 h dark photoperiod for 3 weeks.

## Experiment 2 and 3: Flow Velocity and Irradiance

This experiment was designed to test the effect of water flow velocity on the  $\text{H}_2\text{O}_2$  concentration of the plant tissues and the interaction with irradiance (Atapaththu and Asaeda, 2015; Asaeda et al., 2017). Two sets of experiments were conducted. In the first experiment, experimental plants (*E. nuttallii*, *P. crispus*, *C. demersum*) were exposed to two water flow levels (16 and 25 cm/s) using custom-made recirculating flumes (dimensions: 240 cm long  $\times$  25 cm width  $\times$  28 cm depth) exposed to artificial light intensity by the LED lights, or dark conditions. Pre-aerated tap water was circulated by centrifugal electric motor pumps. Pre-acclimatized potted plants were allocated to a section in the flume where water was introduced through a gradually shrinking entrance section to reduce

turbulence. Plants were continuously exposed to low or high mean flow velocities for up to 4 days. During the experiment, mean water flow velocity was detected using an ultrasonic velocimeter (Tokyo Keisoku Co. Ltd., Japan) directly above the plant leaf surface and recorded daily to minimize flow variation. Temperature level was maintained at  $15 \pm 2^{\circ}\text{C}$  using an aquarium water temperature controlling system (Aquarium cooler ZC-100a, Zensui Corporation, Tokyo, Japan). Stress assays by means of  $\text{H}_2\text{O}_2$  measurements were performed every 3 h from 6:00 to 18:00 after 4 days' exposure, and each treatment contained three replicate flumes. For another experiment, a flume channel 2.4 m long, 25 cm wide and 22 cm depth was constructed outdoors. Eighteen flat pots with more than three *E. densa* plants were carefully and randomly installed. Water temperature was kept at  $25 \pm 2^{\circ}\text{C}$  throughout the experiment. Flow velocities from stagnant to 40 cm/s were employed under different solar radiation, and after 3 h, three plants were sampled at each time and a stress assay was conducted immediately. PAR intensity in the water was measured with a portable quantum flux meter (Apogee, MQ-200, United States).

## Field Observations

Several rivers that are highly colonized by *E. densa* were selected from the species distribution database in Japan (MLIT, 2019). The selected rivers were assessed to obtain detailed location information pertaining to the colonization of *E. densa*. Sampling was conducted in the Eno River and its tributary Tajibi River (April, May, and September 2016; April and June 2017); in the Saba River and its tributary Shimaji River (May, June, and September 2016; April and June 2017; August 2018), and in the Hii River (October 2016). At each sampling point, water flow velocity was measured with an ultrasonic velocimeter (Tokyo Keisoku Co. Ltd., Japan) at 20% (reference velocity) and 80% (depth of the colony) of the total water depth (Chow, 2009). PAR intensity in the water was measured with a portable quantum flux meter (Apogee, MQ-200, United States) at 10 cm depth intervals. *M. spicatum* was sampled in the Moto-Arakawa River near Tokyo in April 2015. The river was approximately 5 m wide and 40 cm deep, and the channel slope was approximately 1/1,000. The bottom surface was patchily covered with *M. spicatum*, *E. nuttallii*, *C. demersum*, and *Sparganium* spp. PAR, and velocity distributions were measured with a portable quantum flux meter (Apogee, MQ-200, United States) and an ultra-sonic velocimeter, respectively. *E. nuttallii* was sampled in July and September 2018 from the same river. Sampling was conducted approximately every 3 h in the light-exposed and dark-adapted conditions to remove the effect of solar radiation. The dark treatment involved placing a black plastic sheet ( $3\ \text{m} \times 3\ \text{m}$ ) floating over part of the plant colony for 30 min. The 30 min pre-dark period was determined by laboratory experiments, which were specifically conducted to determine the optimum pre-darkness duration (data not shown). In August 2017, a sampling of *M. spicatum* was conducted in the Sakuradabori of the Imperial Palace Moat, at the center of Tokyo, where *M. spicatum* made a mono-specific stand. The depth of the sampling site was 0.3 m–2.5 m. Both solar-exposed and dark-adapted samples were taken. Plant biomass was sampled from  $50\ \text{cm} \times 50\ \text{cm}$  quadrats in all sampling sites. The

plant samples were placed in plastic bags and immediately stored in a cooling box containing dry ice for transfer to the laboratory where it was stored at  $-80^{\circ}\text{C}$  until an  $\text{H}_2\text{O}_2$  assay and chlorophyll estimation were conducted.

## Determination of Shoot Growth Rate, $\text{H}_2\text{O}_2$ and Chl-a Concentrations

The length of the plants grown in the experimental units was measured using a millimeter scale at 5–7 day intervals. The shoot growth rate (SGR) was calculated as the difference in shoot length between two observations divided by the duration, and it was expressed in cm/day. At the end of each experiment, fresh plant shoots were extracted ( $\sim 500$  mg) in an ice-cold phosphate buffer (50 mM, pH 6.0) that contained polyvinylpyrrolidone (PVP), and the extractions were centrifuged at  $5,000 \times g$  for 20 min at  $4^{\circ}\text{C}$ . This extraction was used to analyze the  $\text{H}_2\text{O}_2$  content spectrophotometrically following the  $\text{TiSO}_4$  method (Satterfield and Bonnell, 1955) with modifications. The reaction mixture contained 750  $\mu\text{l}$  of enzyme extract and 2.5 ml of 1%  $\text{TiSO}_4$  in 20%  $\text{H}_2\text{SO}_4$  (v/v), which was centrifuged at  $5,000 \times g$  for 15 min at  $20^{\circ}\text{C}$ . The optical absorption of the developed yellow color was measured spectrophotometrically at a wavelength of 410 nm. The  $\text{H}_2\text{O}_2$  concentration in samples was determined using the prepared standard curve for known concentration series and was expressed in  $\mu\text{mol}$  per gram fresh weight ( $\mu\text{mol/gFW}$ ).

Chlorophyll *a* (Chl-*a*) concentrations of experimental plants were determined spectrophotometrically (UV Mini 1210, Shimadzu, Japan) by extracting pigments with *N,N*-dimethylformamide after keeping them in darkness for 24 h, and they were expressed in terms of fresh weight (FW) (Wellburn, 1994).

## Statistical Analysis

Data were tested for normality with the Shapiro–Wilk test before statistical analyses. All results were presented as the mean  $\pm$  SD of more than three replicates. Data were subjected to a one-way analysis of variance (ANOVA) with Tukey's *post-hoc* test for mean separation. The *t*-test was performed where necessary. Bivariate analysis was used and followed by Pearson's correlation to evaluate the relationship among parameters. Statistical analyses were performed in IBM SPSS V25.

## Development of the Species-Specific Model to Identify the Colonization Zones

Asaeda et al. (2020) proposed the total  $\text{H}_2\text{O}_2$  concentration formed in plant tissues for a particular temperature (*Temp*) by the sum of  $\text{H}_2\text{O}_2$  generated by metabolism ( $\text{H}_2\text{O}_{2\text{met}}$ ), flow velocity ( $\text{H}_2\text{O}_{2\text{vel}}$ ), and solar radiation ( $\text{H}_2\text{O}_{2\text{rad}}$ ). If the value is between 15 and 20  $\mu\text{mol/gFW}$ , then *E. densa* growth deteriorates.

$$\text{H}_2\text{O}_{2\text{tot}}(\text{Temp}) = \text{H}_2\text{O}_{2\text{rad}}(\text{Temp}) + \text{H}_2\text{O}_{2\text{vel}}(\text{Temp}) + \text{H}_2\text{O}_{2\text{met}}(\text{Temp}) < \text{H}_2\text{O}_{2\text{cr}} (= 15 - 20 \mu\text{mol/gFW for } E. \text{densa}) \quad (1)$$

For other species, empirical formulas obtained by experiments and field observation were introduced to  $\text{H}_2\text{O}_2$  concentrations

generated by each environmental component, solar radiation,  $\text{H}_2\text{O}_{2\text{rad}}(\text{Temp})$ , temperature increment,  $\text{H}_2\text{O}_{2\text{rad}}(\text{Temp})$ , the basal level of the metabolism, the  $\text{H}_2\text{O}_{2\text{met}}(\text{Temp})$  (Apel and Hirt, 2004), and the threshold level to deteriorate,  $\text{H}_2\text{O}_{2\text{cr}}$ .

In rivers flowing with moderate velocity, water is fully mixed. Therefore, the light attenuation coefficient is nearly uniform at all depths, and the light intensity is given by  $I_0 \exp(-kz)$ , where  $I_0$  is the light intensity just below the water surface,  $k (= 0.083 \text{ cm}^{-1})$  is the attenuation constant of light in water, and  $z$  is the canopy depth. The intensity of solar radiation,  $I_0$  ( $\mu\text{mol/m}^2/\text{s}$ ), and water temperature ( $^{\circ}\text{C}$ ) at the Eno and Saba rivers are empirically given as a function of month, *month*:

$$I_0 = 0.93\text{month}^4 - 22.3\text{month}^3 + 134.5\text{month}^2 - 2.22\text{month} + 868 \quad (2)$$

$$\text{Temp} = 0.022\text{month}^4 - 0.66\text{month}^3 + 6.16\text{month}^2 - 17.5\text{month} + 20.4 \quad (3)$$

Flow velocity in a river channel “*Vel*” (cm/s) is estimated by the Manning's equation, assuming the channel is sufficiently wide compared to the depth and is longitudinally uniform, such that:

$$\text{Vel} = \frac{4.63}{n} R^{2/3} S^{1/2} \quad (4)$$

where *R* is the hydraulic radius, approximately given by the depth *H* (cm), *S* is the channel bed slope, and *n* is the Manning's roughness coefficient, where *n* is  $\sim 0.090$  in the river zones considered in the present study (personal information).

## RESULTS

### Empirical Relationships of $\text{H}_2\text{O}_2$ Concentration With Abiotic Factors

Combined effects of temperature and light intensity on  $\text{H}_2\text{O}_2$  formation in macrophyte tissues showed a species-specific response (Figure 1). The basal  $\text{H}_2\text{O}_2$  concentrations were 4.6  $\mu\text{mol/gFW}$  at  $20^{\circ}\text{C}$  for *E. densa* and *E. nuttallii*, and 3.0  $\mu\text{mol/gFW}$  at  $20^{\circ}\text{C}$  for other species, respectively, after being exposed to dark conditions. The increment of  $\text{H}_2\text{O}_2$  driven by the temperature change were  $-0.32 \mu\text{mol/gFW}/^{\circ}\text{C}$  for *E. densa* ( $r = -0.985$ ,  $p < 0.01$ ),  $0.39 \mu\text{mol/gFW}/^{\circ}\text{C}$  for *M. spicatum* ( $r = 0.800$ ,  $p < 0.05$ ),  $0.41 \mu\text{mol/gFW}/^{\circ}\text{C}$  for *C. demersum* ( $r = 0.900$ ,  $p < 0.01$ ),  $0.60 \mu\text{mol/gFW}/^{\circ}\text{C}$  for *P. crispus* ( $r = 0.974$ ,  $p < 0.01$ ), and  $0.48 \mu\text{mol/gFW}/^{\circ}\text{C}$  for *E. nuttallii* ( $r = 0.956$ ,  $p < 0.01$ ), respectively.  $\text{H}_2\text{O}_2$  concentrations of different light intensity groups were plotted nearly in parallel, higher with higher light intensity groups ( $p < 0.05$ ).

Water flow velocity and light intensity had significant impacts on the  $\text{H}_2\text{O}_2$  metabolism in macrophytes. The tissue  $\text{H}_2\text{O}_2$  concentration linearly increased responding to increasing water flow velocity for all these species (Figure 2). The increasing rate of  $\text{H}_2\text{O}_2$  concentration with respect to flow velocity showed no significant difference among species with

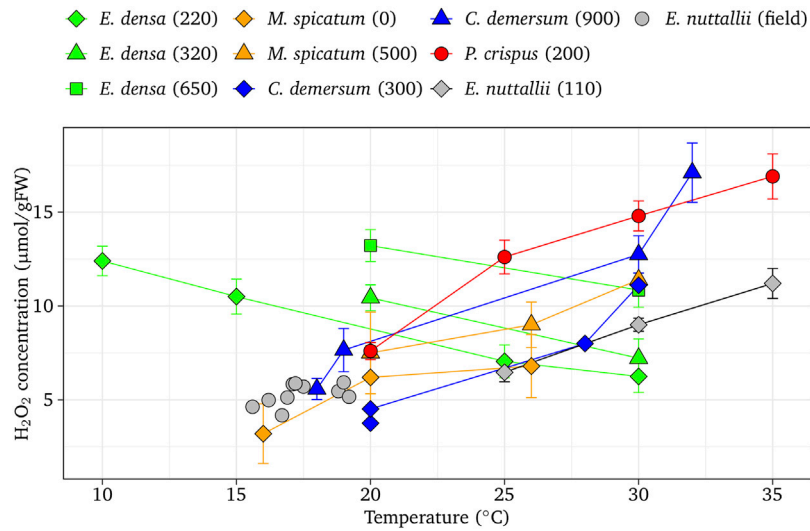


**FIGURE 1** | Effect of temperature on  $H_2O_2$  concentration at different light intensities in native aquatic macrophytes (*M. spicatum*, *C. demersum*, and *P. crispus*) and invasive species (*E. densa* and *E. nuttallii*). Vertical bars indicate the standard deviation. The values in parentheses are light intensities ( $\mu\text{mol}/\text{m}^2/\text{s}$ ).

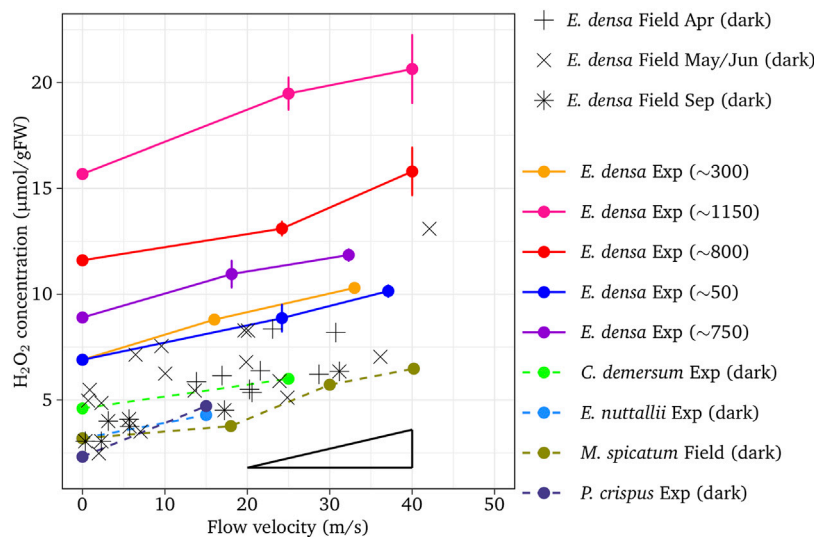


**FIGURE 2** | Effect of flow velocity on  $H_2O_2$  concentration with different light intensities or different sampling time. Vertical bars indicate standard deviation. The triangle shows the average gradient. The values in the parentheses are light intensities ( $\mu\text{mol}/\text{m}^2/\text{s}$ ).

the gradient due to the velocity of  $0.09 H_2O_2/\text{velocity}$  ( $\mu\text{mol}/\text{gFW}/\text{cm}/\text{s}$ ) ( $r = 0.921$ ,  $p < 0.01$  for *E. densa*,  $0.878$ ,  $p < 0.01$  for *E. nuttallii*,  $r = 0.875$ ,  $p < 0.01$  for *P. crispus*,  $r = 0.700$ ,  $p < 0.01$  for *C. demersum* and  $r = 0.957$ ,  $p < 0.01$  for *M. spicatum*). It was similar to the results of field samples,  $0.072 H_2O_2/\text{velocity}$  ( $\mu\text{mol}/\text{gFW}/\text{cm}/\text{s}$ ) as shown in the figure. No significant difference was obtained among the sampling seasons. For *E. densa*,  $H_2O_2$  concentrations for different light intensity groups were plotted nearly in parallel, higher with higher light intensity groups ( $p < 0.01$ ). The increments of  $H_2O_2$  concentrations for the light-exposed samples with respect to the dark-adapted ones are

shown in **Figure 3**. Experimental samples of *E. densa* had a similar increasing trend with field observation in  $H_2O_2$  concentration.

From the field data, Asaeda et al. (2020) derived the following relationship for *E. densa*:

$$H_2O_2_{rad}(Temp) = \frac{[I_0 e^{(-kz)} - 40]^{\frac{2}{3}}}{10} \text{ for } I_0 e^{(-kz)} \geq 40 \mu\text{mol}/\text{m}^2/\text{s}$$

$$\text{for } I_0 e^{(-kz)} < 40 \mu\text{mol}/\text{m}^2/\text{s} \quad (5)$$

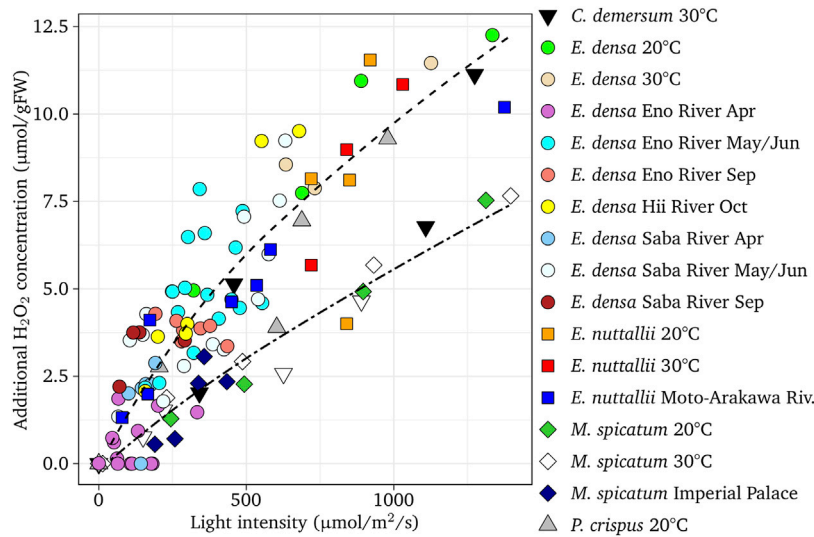


**FIGURE 3** | Additional  $H_2O_2$  concentration of light-exposed tissues with respect to dark-adapted ones of different rivers and experiments as a function of the light intensity for different species. The regression curves,  $H_2O_2 = [\text{light intensity} - 40]^{2/3} / 10$  (upper dotted curve) and  $H_2O_2 = [\text{light intensity} - 40]^{5/6} / 55$  (lower dotted curve) are presented. Field samples of *E. densa* (Asaeda et al., 2020) are shown for comparison.

**Figure 3** indicates that a similar relationship is available for *E. nuttallii* and *P. crispus* without a large error ( $r = 0.97$ ,  $p < 0.01$  for *E. nuttallii* and  $r = 0.99$ ,  $p < 0.01$ , respectively). For *M. spicatum* and *C. demersum*, the increasing rate of  $H_2O_2$  with respect to solar radiation was slightly lower, decreasing the effect of the solar radiation. Therefore, a different equation was derived for *M. spicatum*, and *C. demersum* ( $r = 0.98$ ,  $p < 0.01$  for *M. spicatum*, and  $r = 0.89$ ,  $p < 0.01$  for *C. demersum*, respectively).

$$H_2O_{2\ rad}(Temp) = \frac{[I_0 e^{(-kz)} - 40]^{5/6}}{55} \quad \text{for } I_0 e^{(-kz)} \geq 40 \text{ } \mu\text{mol/m}^2/\text{s}$$

$$H_2O_{2\ rad}(Temp) = 0 \quad \text{for } I_0 e^{(-kz)} < 40 \text{ } \mu\text{mol/m}^2/\text{s}$$

(6)

## The Threshold $H_2O_2$ Concentration for Growth Deterioration

Chl-a concentrations and SGR as functions of  $H_2O_2$  concentrations at different flow velocities, water temperatures, and light intensities of *E. densa* are shown in **Figure 4A**. Regardless of environmental factors, both Chl-a concentrations and SGR decreased with increasing  $H_2O_2$  concentrations (flow velocity  $r = -0.944$ ,  $p < 0.01$  for Chl-a and  $r = -0.964$ ,  $p < 0.01$  for SGR; temperature  $r = -0.945$ ,  $p < 0.01$  for Chl-a and  $r = -0.980$ ,  $p < 0.01$  for SGR; light  $r = -0.924$ ,  $p < 0.01$  for Chl-a and  $r = -0.965$ ,  $p < 0.01$  for SGR). **Figure 4B** presents the relationships of  $H_2O_2$  and Chl-a concentrations for *M. spicatum*, *C. demersum*, *E. nuttallii*, and *P. crispus*. Chl-a concentration decreased with the  $H_2O_2$  concentration ( $r = -0.896$ ,  $p < 0.01$  for *M. spicatum*,  $r = -0.752$ ,  $p < 0.01$  for *C. demersum*,  $r = -0.497$ ,  $p < 0.01$  for *E.*

*nuttallii*, and  $r = -0.963$ ,  $p < 0.01$  for *P. crispus*), and was eliminated at approximately 16–20  $\mu\text{mol/gFW}$ . In the field observation, tissue deterioration occurred when similar  $H_2O_2$  concentrations continued for a few days.

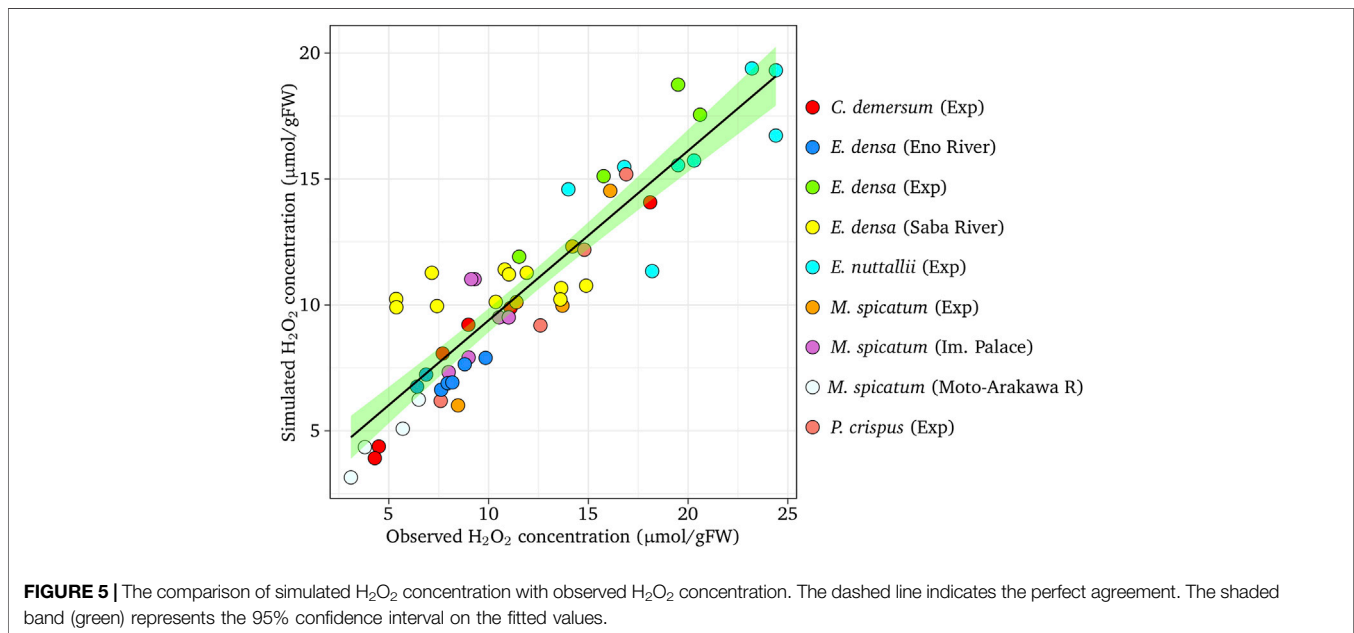
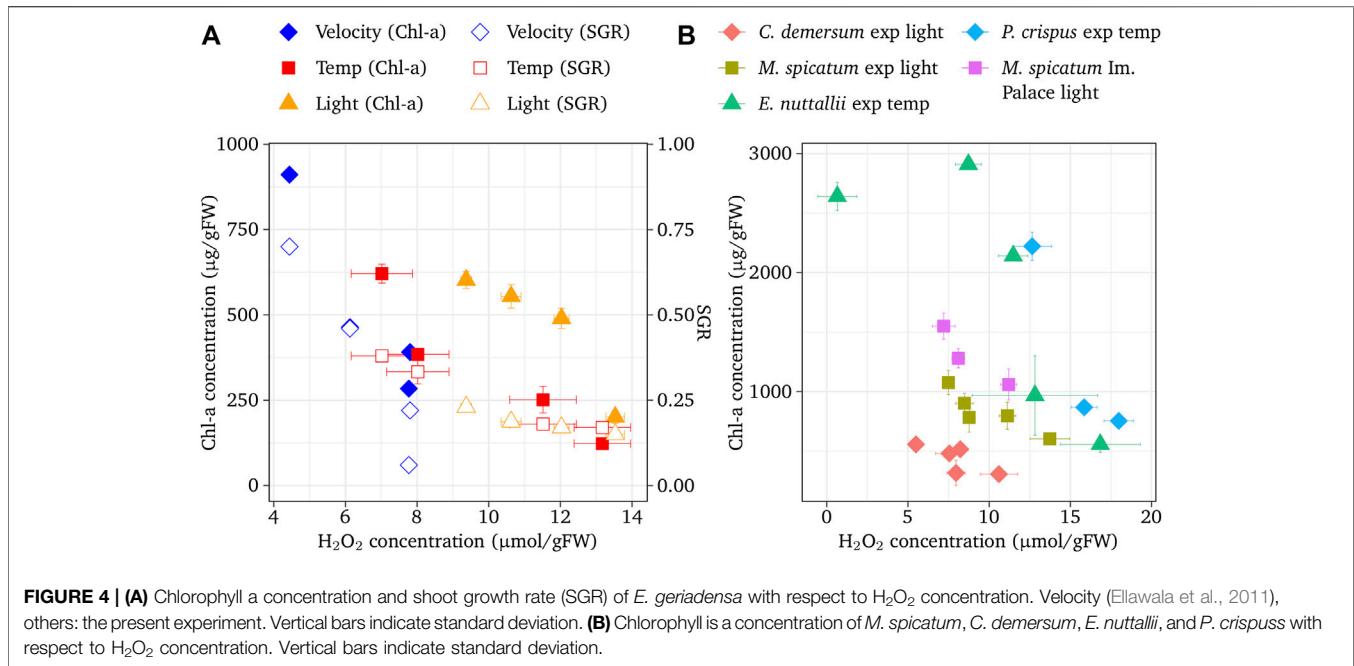
## Simulated Results

### The Comparison With the Observed Data

**Figure 5** shows the comparison between the observed  $H_2O_2$  concentration and simulated  $H_2O_2$  concentration for experimental and observed results. Satisfactory agreement between the simulated and observed values were found in the simulation ( $r = 0.798$ ,  $p < 0.01$  for *E. densa*,  $r = 0.700$ ,  $p < 0.05$  for *E. nuttallii*,  $r = 0.919$ ,  $p < 0.01$  for *M. spicatum*,  $r = 0.976$ ,  $p < 0.01$  for *C. demersum*, and  $r = 0.974$ ,  $p < 0.05$  *P. spicatum*).

### The Depth-Wise Distribution of $H_2O_2$ Concentration of Different Species

The  $H_2O_2$  concentration of *E. densa* was simulated for channel slopes of 1/300 at 10, 20, and 30°C, which were close to the condition of the observed reaches of the Eno and the Saba rivers in March, May/June, and October as well as August to September, respectively. **Figure 6** shows the simulated results with respect to the depth, observed  $H_2O_2$ , and macrophyte biomass. The threshold  $H_2O_2$  concentration was assumed as 16  $\mu\text{mol/gFW}$ . The  $H_2O_2$  concentration was high at the water surface and gradually decreased. With deeper depth, increasing velocity increases the  $H_2O_2$  concentration. The decreasing or increasing trend with respect to depth depends on the combination of these two factors. The  $H_2O_2$  concentration of the stagnant water is lower than the sloped channel, as  $H_2O_2$  generated by the velocity is zero. In the case of *E. densa*, the  $H_2O_2$  concentration is higher with lower temperature, and



mostly above the threshold value at  $10^{\circ}C$ , indicating the colonization is limited. The observed  $H_2O_2$  concentrations were plotted within  $2 \mu\text{mol/gFW}$  from the simulated corresponding temperature line. All the biomass data were plotted in the depth where the  $H_2O_2$  line of the corresponding temperature was below the threshold value. The simulated results agreed with the field sampling. The  $H_2O_2$  concentration was simulated for *M. spicatum*; *C. demersum*, *P. crispus*, and *E. nuttallii* were compared to the

observed  $H_2O_2$  values and biomass in the field (**Figures 7–9**). Both the  $H_2O_2$  concentration and the existing biomass range agreed well with observed data ( $H_2O_2$  concentration: within  $2.5 \mu\text{mol/gFW}$ , all positive biomass range was in the range where the  $H_2O_2$  values were below the threshold). The  $H_2O_2$  concentration of these species increases with increasing temperature. The  $H_2O_2$  concentration is higher at the shallow zone; thus, the total  $H_2O_2$  concentration exceeds the threshold value.

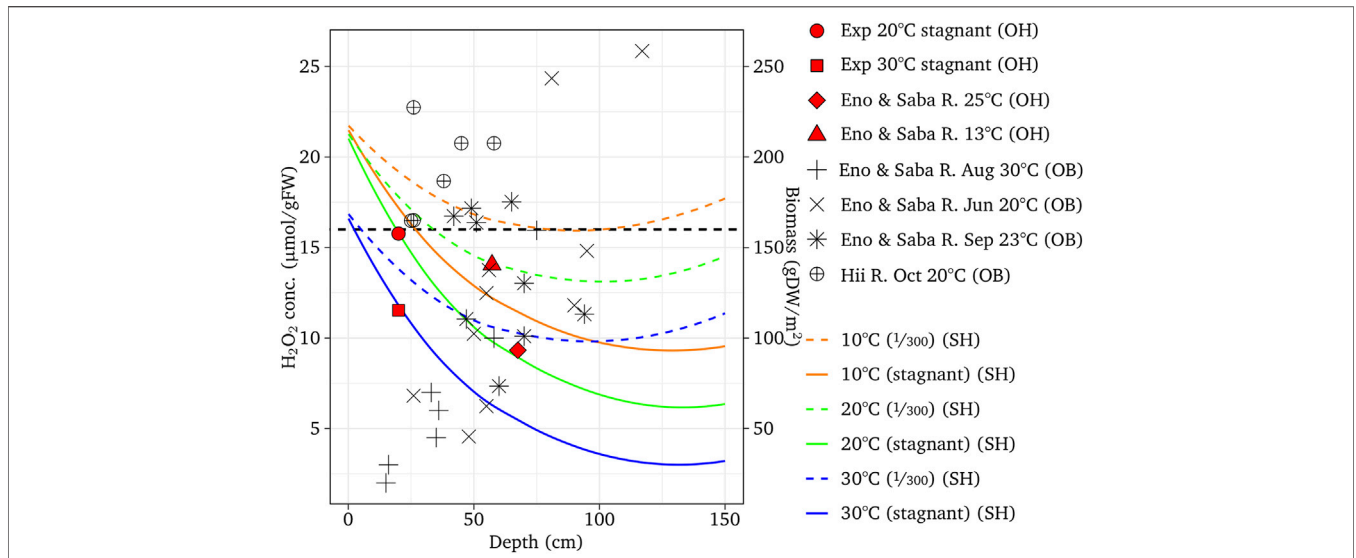


**FIGURE 6** | Simulated  $H_2O_2$  concentration with respect to the river depth for the channel slopes of 1/300 or stagnant water condition, and different temperature, compared with the  $H_2O_2$  concentration and biomass of experiments at the Eno and Saba rivers. ‘OH’, ‘OB’ and ‘SH’ designate observed  $H_2O_2$ , observed biomass, and simulated  $H_2O_2$ , respectively.

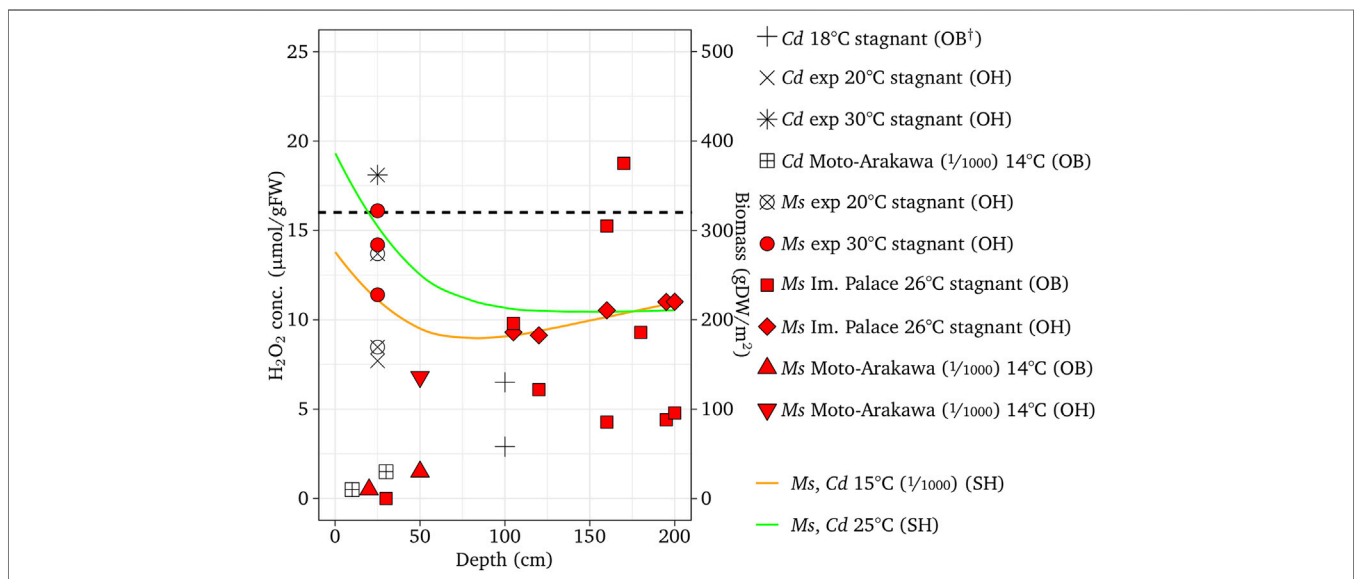


**FIGURE 7** | Simulated  $H_2O_2$  concentrations with different temperatures compared with the observed results for *M. spicatum* (Ms in the legend) and *C. demersum* (Cd in the legend) compared with observed data. † Represents Fukuhara et al. (1997); ‘OB’, ‘SH’ and ‘SH’ designate observed biomass, observed  $H_2O_2$  and simulated  $H_2O_2$ , respectively. The fractions in the parentheses are channel slopes.

### The Composition of the $H_2O_2$ Component for Different Types of Rivers

Figure 10 presents the simulated results of  $H_2O_2$  fractions generated by environmental conditions: temperature-dependent metabolism ( $H_2O_{2met}(Temp)$ ), solar radiation ( $H_2O_{2rad}$ ), velocity,  $H_2O_{2vel}$  for a 0.4 m deep (*E. densa* and *M. spicatum*), and colonized and non-colonized rivers. A 5 year average of monthly temperatures was used for the Eno and the Saba rivers, where *E. densa* are colonized, and for the Arakawa

River and the Tone River in the Tokyo metropolitan area, where no *E. densa* colonies were recorded while *M. spicatum* was colonized (MLIT, 2019). The former groups are slightly warmer than the latter. The total  $H_2O_2$  concentration without a velocity component is available to estimate for stagnant water. At >1 m depth, the  $H_2O_2$  fraction for the solar radiation was almost nil. The increment of  $H_2O_2$  concentration due to increasing temperatures after spring has opposite trends between *E. densa* and *M. spicatum*; the  $H_2O_2$  concentration decreased with *E. densa* and increased with



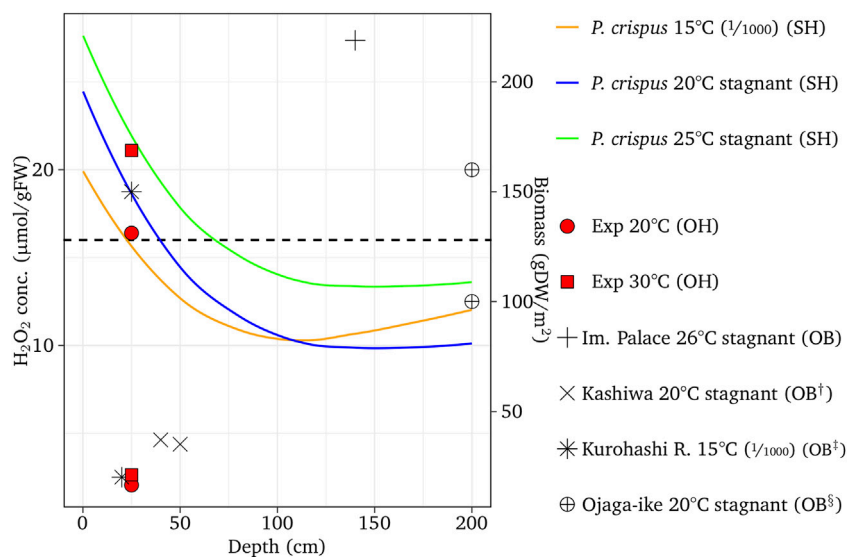


**FIGURE 8 |** Simulated  $\text{H}_2\text{O}_2$  concentrations with different temperatures compared with the observed results for *P. crispus* compared with observed data. 'OH', 'SH' and 'OB' designate observed  $\text{H}_2\text{O}_2$ , simulated  $\text{H}_2\text{O}_2$ , and observed biomass, respectively. †, ‡ and § designate Shinohara et al. (2014), Takahashi and Asaeda (2014), and Kunii (1984), respectively. The fractions in the parentheses are channel slopes.

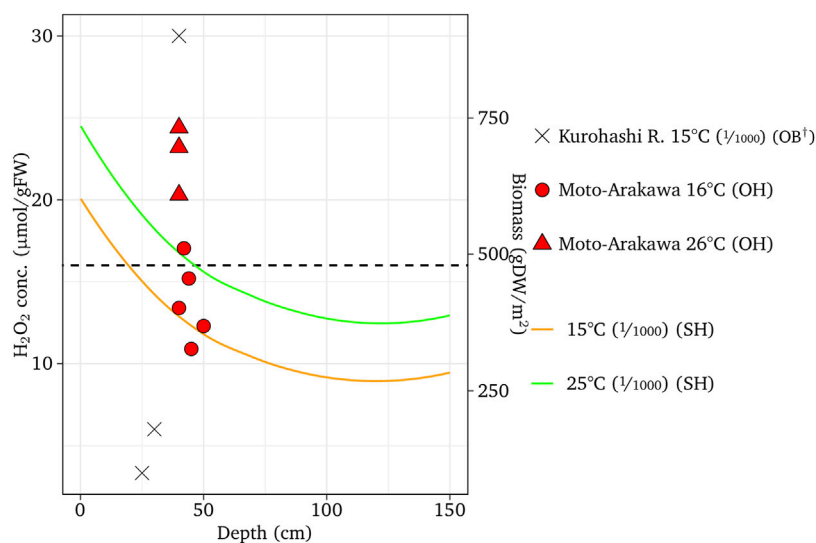


**FIGURE 9 |** Simulated  $\text{H}_2\text{O}_2$  concentrations with different temperatures compared with the observed results for *E. nuttallii* compared with observed data. † = Takahashi et al. (2014); 'OH' and 'SH' designate observed and simulated  $\text{H}_2\text{O}_2$ , respectively. The fractions in the parentheses are channel slopes.

*M. spicatum*. Temperature was the most effective component to differentiate the annual patterns of the total  $\text{H}_2\text{O}_2$  concentration. The fraction of  $\text{H}_2\text{O}_2$  due to solar radiation was higher for *E. densa* than for *M. spicatum*; thus, *E. densa* colonization was highly affected by solar radiation. For *E. densa*, the  $\text{H}_2\text{O}_2$  concentration maintained higher than the threshold value until June in the colder group of rivers, but it becomes lower than the threshold from April/May in the warmer group. For *M. spicatum*, on the other hand, the total  $\text{H}_2\text{O}_2$  concentration exceeded the threshold value from April in the warmer group while only in August in the colder group. In the

stagnant water, the total  $\text{H}_2\text{O}_2$  concentration of *M. spicatum* exceeded the threshold value in summer.

## DISCUSSION

### Tissue $\text{H}_2\text{O}_2$ Concentration as Affected by Environmental Conditions

Previous studies have shown that  $\text{H}_2\text{O}_2$  concentration of the plant tissues increases in unpreferable environmental conditions

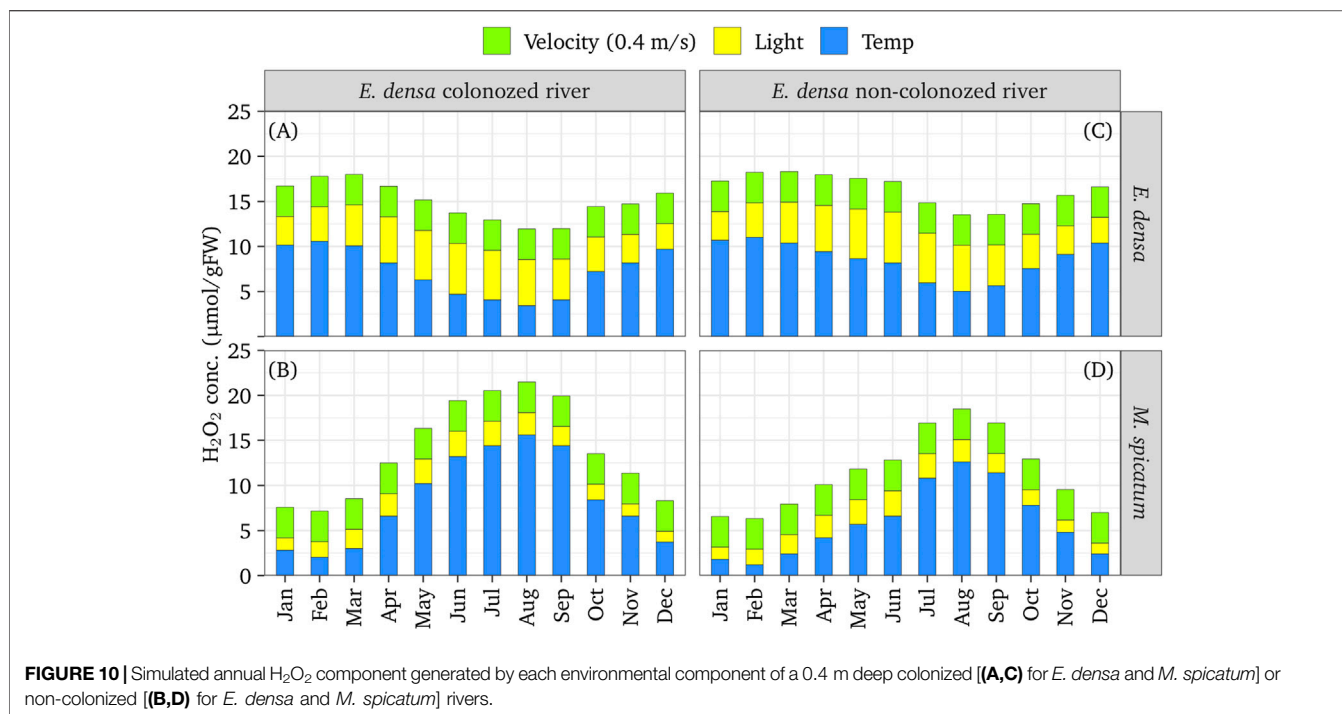


**FIGURE 10** | Simulated annual H<sub>2</sub>O<sub>2</sub> component generated by each environmental component of a 0.4 m deep colonized [(A,C) for *E. densa* and *M. spicatum*] or non-colonized [(B,D) for *E. densa* and *M. spicatum*] rivers.

(Asaeda et al., 2020; Elsheery et al., 2020a; Elsheery et al., 2020b), and it is highly correlated with the intensity of a single environmental factor (Asaeda et al., 2017; Asaeda and Sanjaya, 2017; El-Sheery, 2017; Parveen et al., 2017; Chalanika De Silva and Asaeda, 2018). The present study elucidates that under a combination of different environmental factors, the total H<sub>2</sub>O<sub>2</sub> concentration is provided as the sum of H<sub>2</sub>O<sub>2</sub> generated by individual factors and the amount generated by metabolism (Apel and Hirt, 2004). In addition, the relationship between H<sub>2</sub>O<sub>2</sub> concentration and the intensity of each environmental factor does not vary much between seasons and phenological stages of the plant (Asaeda et al., 2020). Therefore, the H<sub>2</sub>O<sub>2</sub> concentration is considered an indicator of the degree of the unpreferable condition. The Chl-a concentration and the growth parameter decreased with increasing intensity of the total H<sub>2</sub>O<sub>2</sub> concentration (Coleman et al., 1989; French and Moore, 2003; Boustany et al., 2010). Interestingly, when the tissue H<sub>2</sub>O<sub>2</sub> concentration exceeded 16–20 µmol/gFW, the plants became brownish and deteriorated. Therefore, the environmental conditions reflected by H<sub>2</sub>O<sub>2</sub> concentrations below this threshold allows macrophytes to form a large and healthy colony. This system can be applied to elucidate the growth area of macrophyte species, by formulating the H<sub>2</sub>O<sub>2</sub> concentrations and abiotic conditions in the environment.

## Environmental Conditions Influencing Macrophyte Colonization in Japanese Rivers

In Japanese rivers, the water quality is relatively good and there is no salinity in the midstream (Luo et al., 2011). Organic matter accumulates on the bottom in stagnant zones, which creates an

anoxic zone in the sediment layer. There are such areas in the lowland zones; however, anoxia of the bottom sediment contributed only ~3 µmol/gFW of H<sub>2</sub>O<sub>2</sub> (Parveen et al., 2017). Chalanika De Silva and Asaeda (2018) showed that the H<sub>2</sub>O<sub>2</sub> concentration differs between mono- and mixed-cultures of species in stagnant water, indicating the effect of species competition. However, the difference was only ~2 µmol/gFW. In field sampling, Japanese native species, *P. crispus* and *C. demersum*, were often found in thick *E. densa* colonies due to the reduction of flow velocity inside the colony (20 cm/s inside compared to 50 cm/s outside, according to our own observation). This indicates that the increment of H<sub>2</sub>O<sub>2</sub> concentration due to competition is less than the reduction of velocity-induced H<sub>2</sub>O<sub>2</sub> (~3 µmol/gFW). In this study, the H<sub>2</sub>O<sub>2</sub> concentrations attributed to water temperature, high solar radiation, and high flow velocities of natural conditions are ~10, ~10, and ~5 µmol/gFW, respectively. Therefore, water temperature, solar radiation and flow velocity are the major dominant environmental factors determining the colonization patterns of macrophytes in the midstream of Japanese rivers.

## Species-Specific Trait of H<sub>2</sub>O<sub>2</sub> Concentration in Response to Environmental Conditions

Laboratory and field experiments showed a typical species-specific relationship between H<sub>2</sub>O<sub>2</sub> concentration and the environmental factors of temperature, flow velocity, and solar radiation. With increasing flow velocity, the similar increasing trend of H<sub>2</sub>O<sub>2</sub> concentration was obtained for all tested species. Although flow velocity generates a large amount of H<sub>2</sub>O<sub>2</sub>, it does not affect the dominance of a particular species. High solar

radiation intensively generates  $H_2O_2$  (Asada, 2006). Specifically, the  $H_2O_2$  concentrations of *E. densa* and *E. nuttallii* were  $\sim 10 \mu\text{mol/gFW}$  under the daily highest solar radiation, which were much higher than those of Japanese native species, *M. spicatum* and *C. demersum*, which were  $\sim 6 \mu\text{mol/gFW}$ . This impacts the ability of *E. densa* to colonize in the shallow zone, where the solar radiation is high; thus, *E. densa* was found to colonize in relatively deep zones ( $<30 \text{ cm}$  deep). Japanese native species were, on the other hand, often found at shoreline or close to the water surface. There was an opposite trend in  $H_2O_2$  concentrations for water temperature between *E. densa* and other species. With *E. densa*,  $H_2O_2$  concentration decreased with increasing temperature, while major Japanese native species, *M. spicatum*, *C. demersum*, and *P. spicatum* as well as another invasive species, *E. nuttallii*, showed an increasing trend of  $H_2O_2$  concentration with temperature. The different trends between Japanese native species and *E. densa* are reflected to their phenology and colonization area.

### Possible Reason for the Overproduction of *E. densa* in Japanese Rivers

Low water temperature increases *E. densa*  $H_2O_2$  concentration. In rivers where *E. densa* colonized overwhelmingly, water temperature decreases below  $8^\circ\text{C}$  in winter. However, even at that time,  $H_2O_2$  concentration remains below the threshold value at around 1 m deep in stagnant water. Small patchy colonies were found in the upstream of weirs. With increasing temperatures in spring, they started to grow and form a large summer colony, expanding to a shallow zone in the downstream. The channels were originally covered with gravel bed; the bed morphology easily changed under high flow and pools disappeared. However, river rehabilitation for the flood control has been intensively conducted in the last five decades. The shallow zone of the channels was excavated to deepen the channel, and *E. densa* can now colonize with low  $H_2O_2$  concentration. Weirs were constructed frequently, which created deep stagnant water in the upstream. Thus, the  $H_2O_2$  concentration of *E. densa* due to velocity and solar radiation may decrease. Gravel mining was conducted, substantially reducing the amount of gravel in the river channel, and there is no longer any sediment transport even at flood time (Asaeda and Sanjaya, 2017). Thus, the modified river morphology does not change even during floods. The artificially created deep zone became a trigger for the overproduction of *E. densa* in the river channel. In the last three decades, river water temperature has significantly increased due to global warming at approximately  $0.1^\circ\text{C}/\text{year}$ , often reaching  $30^\circ\text{C}$ , particularly in western Japanese rivers (Ministry of Environment, 2013). It seems difficult for Japanese native species and *E. nuttallii* to grow in these rivers. Particularly, *E. densa* and *E. nuttallii* are closely related species and came to Japan at nearly the same time. However, the overwhelming colonization of *E. densa* and the limitations of *E. nuttallii* seem to be attributed to the different temperature traits of these species. Local people emphasize the recent reduction of flow rate (personal communication). During

the day, in addition to high solar radiation, water temperature is approximately  $2^\circ\text{C}$  higher than at night, particularly under a low summer flow rate. Thus, during this time, both solar radiation and temperature increases the  $H_2O_2$  concentration for Japanese native species. However, their effects are reciprocal and do not affect *E. densa* very much. It is likely another reason for the overwhelming presence of *E. densa*.

## CONCLUSION

Under unpreferable environmental conditions,  $H_2O_2$  concentrations increase in plant tissues and reflect the macrophyte condition fairly accurately. Potentially, this could be a good indicator of submerged macrophyte colonization. This approach will save time by not requiring casual observations and biomass monitoring of macrophytes in ecosystem monitoring. The experimental and field observations indicated a clear positive relationship between the level of unpreferable conditions and  $H_2O_2$  concentrations, regardless of abiotic factors. The total  $H_2O_2$  concentration is provided by the sum of  $H_2O_2$  generated by each environmental factor, and  $<16\text{--}20 \mu\text{mol/gFW}$  is required for colonization. The relationships of  $H_2O_2$  concentrations and the contribution of each abiotic factor were obtained for invasive species (*E. densa* and *E. nuttallii*) and three major Japanese native species (*M. spicatum*, *C. demersum*, and *P. crispus*). The system was applied to develop a mathematical model to simulate the colonization area of these species. The tissue  $H_2O_2$  concentration decreases with increasing temperature for *E. densa* and increases for other species, including native species. Therefore, native species grow intensively in spring; however, they often deteriorate in summer. For *E. densa*, on the other hand,  $H_2O_2$  concentration decreases with high water temperatures in summer, allowing intensive growth. High solar radiation increases the  $H_2O_2$  concentration, deteriorating the plant. Although the  $H_2O_2$  concentration of *E. densa* increases with low water temperatures in winter, it can survive in deep water with low  $H_2O_2$  concentration due to solar radiation. Currently, river rehabilitation has created a deep zone in the channel, which has supported the growth and spread of *E. densa*.

## DATA AVAILABILITY STATEMENT

The datasets generated for this study are available on request to the corresponding author.

## AUTHOR CONTRIBUTIONS

TA: contributed the conceptualization and field work, and wrote the manuscript together with other members; MR: contributed to field sampling, laboratory and data analyses, and helped write the manuscript; JS: reviewed and commented on the manuscript.

## FUNDING

This work was financially supported by the Grant-in-Aid for Scientific Research (B) (19H02245) and Fund for the Promotion of Joint International Research (18KK0116) of Japan Society for the Promotion of Science (JSPS).

## REFERENCES

- Apel, K., and Hirt, H. (2004). Reactive oxygen species: metabolism, oxidative stress, and signal transduction. *Annu. Rev. Plant Biol.* 55, 373–399. doi:10.1146/annurev.arplant.55.031903.141701
- Asada, K. (2006). Production and scavenging of reactive oxygen species in chloroplasts and their functions. *Plant Physiol.* 141, 391. doi:10.1104/pp.106.082040
- Asaeda, T., Rashid, M. H., Dong, M., and Uddin, F. (2013). “The most effective factors responsible for increase in the vegetation coverage of river channels,” in Proceedings of the 35th IAHR Biennial Congress, Chengdu, China, September 8–13, 2013, 17.
- Asaeda, T., and Sanjaya, K. (2017). The effect of the shortage of gravel sediment in midstream river channels on riparian vegetation cover. *River Res. Appl.* 33, 1107–1118. doi:10.1002/rra.3166
- Asaeda, T., Sanjaya, K., and Kaneko, Y. (2017). Effects of mechanical stressors caused by mean flow and turbulence on aquatic plants with different morphologies. *Ecohydrology* 10, e1873. doi:10.1002/eco.1873
- Asaeda, T., Senavirathna, M. D. H., and Vamsi Krishna, L. (2020). Evaluation of habitat preferences of invasive macrophyte *Egeria densa* in different channel slopes using hydrogen peroxide as an indicator. *Front. Plant. Sci.* 11, 422. doi:10.3389/fpls.2020.00422
- Asaeda, T., Senavirathna, M. D. H., Xia, L. P., and Barnuevo, A. (2018). Application of hydrogen peroxide as an environmental stress indicator for vegetation management. *Engineering* 4, 610–616. doi:10.1016/j.eng.2018.09.001
- Atapaththu, K. S., Miyagi, A., Atsuzawa, K., Kaneko, Y., Kawai-Yamada, M., and Asaeda, T. (2015). Effects of water turbulence on variations in cell ultrastructure and metabolism of amino acids in the submersed macrophyte, *Elodea nuttallii* (Planch.) H. St. John. *Plant Biol. (Stuttg.)* 17, 997–1004. doi:10.1111/plb.12346
- Atapaththu, K. S. S., and Asaeda, T. (2015). Growth and stress responses of Nuttall’s waterweed *Elodea nuttallii* (Planch) St. John to water movements. *Hydrobiologia* 747, 217–233. doi:10.1007/s10750-014-2141-9
- Barko, J. W., Gunnison, D., and Carpenter, S. R. (1991). Sediment interactions with submersed macrophyte growth and community dynamics. *Aquat. Bot.* 41, 41–65. doi:10.1016/0304-3770(91)90038-7
- Bates, A. E., Mckelvie, C. M., Sorte, C. J., Morley, S. A., Jones, N. A., Mondon, J. A., et al. (2013). Geographical range, heat tolerance and invasion success in aquatic species. *Proc. Biol. Sci.* 280, 20131958. doi:10.1098/rspb.2013.1958
- Boano, F., Harvey, J. W., Marion, A., Packman, A. I., Revelli, R., Ridolfi, L., et al. (2014). Hyporheic flow and transport processes: mechanisms, models, and biogeochemical implications. *Rev. Geophys.* 52, 603–679. doi:10.1002/2012RG000417
- Boustany, R. G., Michot, T. C., and Moss, R. F. (2010). Effects of salinity and light on biomass and growth of *Vallisneria americana* from Lower St. Johns River, FL, USA. *Wetl. Ecol. Manag.* 18, 203–217. doi:10.1007/s11273-009-9160-8
- Chalanika De Silva, H. C., and Asaeda, T. (2018). Stress response and tolerance of the submersed macrophyte *Elodea nuttallii* (Planch) St. John to heat stress: a comparative study of shock heat stress and gradual heat stress. *Plant Biosyst.* 152, 787–794. doi:10.1080/11263504.2017.1338628
- Choudhury, F. K., Rivero, R. M., Blumwald, E., and Mittler, R. (2017). Reactive oxygen species, abiotic stress and stress combination. *Plant J.* 90, 856–867. doi:10.1111/tpj.13299
- Chow, V. T. (2009). *Open channel hydraulics*. Caldwell, NJ: Blackburn Press.
- Coleman, J. S., Mooney, H. A., and Gorham, J. N. (1989). Effects of multiple stresses on radish growth and resource allocation: I. Responses of wild radish plants to a combination of SO<sub>2</sub> exposure and decreasing nitrate availability. *Oecologia* 81, 124–131. doi:10.1007/BF00377021

## ACKNOWLEDGMENTS

We thank Keerthi Atapaththu, Abner Barnuevo, Lekkala Vamshi Krishna, De Silva Chandani Chalanika, Li-Ping Xia, Akihiko Matsuo, and Viraj Ranawaka for their field sampling and experiments.

- Das, K., and Roychoudhury, A. (2014). Reactive oxygen species (ROS) and response of antioxidants as ROS-scavengers during environmental stress in plants. *Front. Environ. Sci.* 2, 53. doi:10.3389/fenvs.2014.00053
- Dumont, S., and Rivoal, J. (2019). Consequences of oxidative stress on plant glycolytic and respiratory metabolism. *Front. Plant Sci.* 10, 166. doi:10.3389/fpls.2019.00166
- El-Sheery, I. (2017). Effectiveness of potassium silicate in suppression white rot disease and enhancement physiological resistance of onion plants, and its role on the soil microbial community. *Middle East J. G* (2), 376–394. doi:10.1011/s11738-008-0182-x
- Ellawala, C., Kankanamge Asaeda, T., and Kawamura, K. (2011). The effect of flow turbulence on plant growth and several growth regulators in *Egeria densa* Planchon. *Flora* 206, 1085–1091. doi:10.1016/j.flora.2011.07.014
- Elsheery, N. I., Helaly, M. N., El-Hoseiny, H. M., and Alam-Eldein, S. M. (2020a). Zinc oxide and silicone nanoparticles to improve the resistance mechanism and annual productivity of salt-stressed mango trees. *Agronomy* 10 (4), 558. doi:10.3390/agronomy10040558
- Elsheery, N. I., Helaly, M. N., Omar, S. A., John, S. V., Zabochnicka-Swiątek, M., Kalaji, H. M., et al. (2020b). Physiological and molecular mechanisms of salinity tolerance in grafted cucumber. *S. Afr. J. Bot.* 130, 90–102. doi:10.1016/j.sajb.2019.12.014
- French, G. T., and Moore, K. A. (2003). Interactive effects of light and salinity stress on the growth, reproduction, and photosynthetic capabilities of *Vallisneria americana* (wild celery). *Estuaries* 26, 1255. doi:10.1007/BF02803628
- Fukuhara, H., Tanaka, T., and Izumi, M. (1997). Growth and turion formation of *Ceratophyllum demersum* in a shallow lake in Japan. *Jpn. J. Limnol.* 58, 335–347.
- Hauer, F. R., Locke, H., Dreitz, V. J., Hebblewhite, M., Lowe, W. H., Muhlfeld, C. C., et al. (2016). Gravel-bed river floodplains are the ecological nexus of glaciated mountain landscapes. *Sci. Adv.* 2, e1600026. doi:10.1126/sciadv.1600026
- Helaly, M. N., El-Hoseiny, H., El-Sheery, N. I., Rastogi, A., and Kalaji, H. M. (2017). Regulation and physiological role of silicon in alleviating drought stress of mango. *Plant Physiol. Biochem.* 118, 31–44. doi:10.1016/j.plaphy.2017.05.021
- Kadono, Y. (2004). Alien aquatic plants naturalized in Japan: history and present status. *Glob. Environ. Res.* 8, 163–169.
- Kawanabe, H. (1970). Social behaviour and production of ayu-fish in the River Ukawa between 1955 and 1969, with reference to the stability of its territoriality. *Jap. J. Ecol.* 20, 144–151 (in Japanese). doi:10.18960/seitai.20.4\_144
- Kunii, H. (1982). Life cycle and growth of *Potamogeton crispus* L. in a shallow pond Ojaga-Ike. *Bot. Mag. (Tokyo)* 95, 109–124. doi:10.1007/BF02488578
- Kunii, H. (1984). Seasonal growth and profile structure development of *Elodea nuttallii* (Planch.) St. John in pond Ojaga-Ike, Japan. *Aquat. Bot.* 18, 239–247. doi:10.1016/0304-3770(84)90065-2
- Lougheed, V. L., Crosbie, B., and Chow-Fraser, P. (2001). Primary determinants of macrophyte community structure in 62 marshes across the Great Lakes basin: latitude, land use, and water quality effects. *Can. J. Fish. Aquat. Sci.* 58, 1603–1612. doi:10.1139/cjfas-58-8-1603
- Luo, P., He, B., Takara, K., Razafindrabe, B. H., Nover, D., and Yamashiki, Y. (2011). Spatiotemporal trend analysis of recent river water quality conditions in Japan. *J. Environ. Monit.* 13, 2819–2829. doi:10.1039/c1em10339c
- Madsen, J. D., Chambers, P. A., James, W. F., Koch, E. W., and Westlake, D. F. (2001). The interaction between water movement, sediment dynamics and submersed macrophytes. *Hydrobiologia* 444, 71–84. doi:10.1023/A:1017520800568
- Ministry of Environment (2013). *Report on the effect of the climate change on the water quality*. Tokyo, Japan: Ministry of Environment, 68.
- MLIT (2019). *Ministry of land infrastructure transportation and tourism in Japan, river environmental database*. Available at: <http://mizukoku.nilim.go.jp/knskankyo/> (Accessed October 2019).
- Naser, H. M., Hanan, E. H., Elsheery, N. I., and Kalaji, H. M. (2016). Effect of biofertilizers and putrescine amine on the physiological features and

- productivity of date palm (*Phoenix dactylifera*, L.) grown on reclaimed-salinized soil. *Trees (Berl.)* 30 (4), 1149–1161. doi:10.1007/s00468-016-1353-1
- O'Hare, M. T., Baattrup-Pedersen, A., Baumgarte, I., Freeman, A., Gunn, I. D., Lázár, A. N., et al. (2018). Responses of aquatic plants to eutrophication in rivers: a revised conceptual model. *Front. Plant Sci.* 9, 451. doi:10.3389/fpls.2018.00451
- Omar, S. A., Elsheery, N. I., Kalaji, H. M., Xu, Z. F., Song-Quan, S., Carpentier, R., et al. (2012). Dehydroascorbate reductase and glutathione reductase play an important role in scavenging hydrogen peroxide during natural and artificial dehydration of *Jatropha curcas* seeds. *J. Plant Biol.* 55 (6), 469–480. doi:10.1007/s12374-012-0276-7
- Pandit, A. K. (Editor) (2002). *Natural resources of western Himalaya*. New Delhi, India: Valley Book House.
- Parveen, M., Asaeda, T., and Rashid, M. H. (2017). Hydrogen sulfide induced growth, photosynthesis and biochemical responses in three submerged macrophytes. *Flora* 230, 1–11. doi:10.1016/j.flora.2017.03.005
- Pip, E. (1989). Water temperature and freshwater macrophyte distribution. *Aquat. Bot.* 34, 367–373. doi:10.1016/0304-3770(89)90079-X
- Riis, T., Olesen, B., Clayton, J. S., Lambertini, C., Brix, H., and Sorrell, B. K. (2012). Growth and morphology in relation to temperature and light availability during the establishment of three invasive aquatic plant species. *Aquat. Bot.* 102, 56–64. doi:10.1016/j.aquabot.2012.05.002
- Satterfield, C. N., and Bonnell, A. H. (1955). Interferences in titanium sulfate method for hydrogen peroxide. *Anal. Chem.* 27, 1174–1175. doi:10.1021/ac60103a042
- Schoelynck, J., Bal, K., Verschoren, V., Penning, E., Struyf, E., Bouma, T., et al. (2014). Different morphology of *Nuphar lutea* in two contrasting aquatic environments and its effect on ecosystem engineering. *Earth Surf. Proces. Landf.* 39, 2100–2108. doi:10.1002/esp.3607
- Schoelynck, J., De Groote, T., Bal, K., Vandenbruwaene, W., Meire, P., and Temmerman, S. (2012). Self-organised patchiness and scale-dependent biogeomorphic feedbacks in aquatic river vegetation. *Ecography* 35, 760–768. doi:10.1111/j.1600-0587.2011.07177.x
- Sharma, P., Jha, A. B., Dubey, R. S., and Pessarakli, M. (2012). Reactive oxygen species, oxidative damage, and antioxidative defense mechanism in plants under stressful conditions. *J. Bot.* 26, 2012. doi:10.1155/2012/217037
- Shinohara, R., Asaeda, T., and Isobe, M. (2014). Effects of phytoplankton on the distribution of submerged macrophytes in a small canal. *Landsc. Ecol. Eng.* 10, 115–121. doi:10.1007/s11355-013-0227-6
- Smirnov, N., and Arnaud, D. (2019). Hydrogen peroxide metabolism and functions in plants. *New Phytol.* 221, 1197–1214. doi:10.1111/nph.15488
- Suzuki, N., Rivero, R. M., Shulaev, V., Blumwald, E., and Mittler, R. (2014). Abiotic and biotic stress combinations. *New Phytol.* 203, 32–43. doi:10.1111/nph.12797
- Takahashi, K., and Asaeda, T. (2014). The effect of spring water on the growth of a submerged macrophyte *Egeria densa*. *Landsc. Ecol. Eng.* 10, 99–107. doi:10.1007/s11355-012-0191-6
- Tanida, K. (1984). Larval microlocation on stone faces of *Hydropsyche* species (Insecta: Trichoptera), with a general consideration on the relation of systematic groupings to the ecological and geographical distribution among the Japanese *Hydropsyche* species. *Physiol. Ecol. Jpn.* 21, 115–130.
- Weerakoon, H. P. A. T., Atapaththu, K. S. S., and Asanthi, H. B. (2018). Toxicity evaluation and environmental risk assessment of 2-methyl-4-chlorophenoxy acetic acid (MCPA) on non-target aquatic macrophyte *Hydrilla verticillata*. *Environ. Sci. Pollut. Res. Int.* 25, 30463–30474. doi:10.1007/s11356-018-3013-z
- Wellburn, A. R. (1994). The spectral determination of chlorophylls a and b, as well as total carotenoids, using various solvents with spectrophotometers of different resolution. *J. Plant Physiol.* 144, 307–313. doi:10.1016/S0176-1617(11)81192-2
- Zaman, T., and Asaeda, T. (2013). Effects of NH<sub>4</sub>-N concentrations and gradient redox level on growth and allied biochemical parameters of *Elodea nuttallii* (Planch.). *Flora* 208, 211–219. doi:10.1016/j.flora.2013.02.009
- Zerebecki, R. A., and Sorte, C. J. (2011). Temperature tolerance and stress proteins as mechanisms of invasive species success. *PLoS One* 6, e14806. doi:10.1371/journal.pone.0014806
- Zhou, B., Wang, J., Guo, Z., Tan, H., and Zhu, X. (2006). A simple colorimetric method for determination of hydrogen peroxide in plant tissues. *Plant Growth Regul.* 49, 113–118. doi:10.1007/s10725-006-9000-2

**Conflict of Interest:** Author TA was employed by Hydro Technology Institute of Japan. The remaining authors declare that the research was conducted in the absence of any commercial or financial relationships that could be construed as a potential conflict of interest.

The handling editor is currently organizing a Research Topic with one of the authors JS, and confirms the absence of any other collaboration.

Copyright © 2021 Asaeda, Rashid and Schoelynck. This is an open-access article distributed under the terms of the Creative Commons Attribution License (CC BY). The use, distribution or reproduction in other forums is permitted, provided the original author(s) and the copyright owner(s) are credited and that the original publication in this journal is cited, in accordance with accepted academic practice. No use, distribution or reproduction is permitted which does not comply with these terms.